

The large scale structure in the 3D luminosity-distance space and its cosmological applications

Pengjie Zhang^{1,2,3,4}

¹*Department of Astronomy, School of Physics and Astronomy, Shanghai Jiao Tong University, Shanghai, 200240, China**

²*Tsung-Dao Lee institute, Shanghai, 200240, China*

³*IFSA Collaborative Innovation Center, Shanghai Jiao Tong University, Shanghai 200240, China*

⁴*Shanghai Key Laboratory for Particle Physics and Cosmology, Shanghai 200240, China*

Future gravitational wave (GW) observations are capable of detecting millions of compact star binary mergers in extragalactic galaxies, with 1% luminosity-distance (D_L) measurement accuracy and better than arcminute positioning accuracy. This will open a new window of the large scale structure (LSS) of the universe, in the 3D **luminosity-distance space (LDS)**, instead of the 3D redshift space of galaxy spectroscopic surveys. The baryon acoustic oscillation and the AP test encoded in the LDS LSS constrain the D_L - D_A^{co} (comoving angular diameter distance) relation and therefore the expansion history of the universe. Peculiar velocity induces the LDS distortion, analogous to the redshift space distortion, and allows for a new structure growth measure $f_L\sigma_8$. When the distance duality is enforced ($1+z = D_L/D_A^{\text{co}}$), the LDS LSS by itself determines the redshift to $\sim 1\%$ level accuracy, and alleviates the need of spectroscopic follow-up of GW events. But a more valuable application is to test the distance duality to 1% level accuracy, in combination with conventional BAO and supernovae measurements. This will put stringent constraints on modified gravity models in which the gravitational wave D_L^{GW} deviates from the electromagnetic wave D_L^{EM} . All these applications require no spectroscopic follow-ups.

PACS numbers: 98.80.-k; 98.80.Es; 98.80.Bp; 95.36.+x

Introduction.— Discoveries of gravitational wave (GW) produced by black hole (BH)/neutron star (NS)-BH/NS mergers [1–4] have opened the era of gravitational wave astronomy. These GW events can serve as standard sirens to measure cosmological distance from first principles [5, 6] and therefore avoid various systematics associated with traditional methods. It will then have profound impact on cosmology. However, to fulfill this potential, usually it requires spectroscopic follow-ups to determine redshifts of their host galaxies or electromagnetic counterparts. This will be challenging, for the third generation GW experiments such as the Big Bang Observer (BBO, [7, 8]), and the Einstein Telescope[28], which will detect millions of these GW events. Various alternatives have been proposed to circumvent this stringent need of spectroscopic follow-ups [9–12].

We point out a new possibility to circumvent this challenge. These GW events are hosted by galaxies and are therefore tracers of the large scale structure (LSS). With arcminute positioning accuracy and 1% level accuracy in the luminosity distance D_L determination achievable by BBO, we are able to map the **3D large scale structure in the luminosity-distance space (LDS)**. It is analogous to the redshift space LSS mapped by the conventional spectroscopic redshift surveys of galaxies ($D_L \leftrightarrow z$). Therefore it also contains valuable information of baryon acoustic oscillation (BAO), both across the sky and along the line of sight. As BAO in the redshift

space measures the comoving angular diameter distance D_A^{co} and $H(z) = dz/d\chi$ at given redshift bins, BAO in LDS measures D_A^{co} and $H_L \equiv dD_L/d\chi$ at given D_L bins. Here χ is the comoving radial distance. Both the D_L - D_A^{co} relation and the D_L - H_L relation constrain cosmology (Fig. 1), without the need of redshift. Furthermore, both D_A^{co} and H_L can be converted into cosmological redshift through the distance duality relation $1+z = D_L/D_A^{\text{co}}$. Similar to the redshift space distortion (RSD), peculiar velocity also induces the luminosity-distance space distortion (LDSD). This will enable a new measure of structure growth rate $f_L\sigma_8$, which differs from $f\sigma_8$ measured in RSD by a redshift dependent factor.

The luminosity-distance space LSS.— Each GW event provides a 3D position ($D_L^{\text{obs}}, \hat{n}$). With millions of them, arcminute positioning accuracy, and $\mathcal{O}(1\%)$ accuracy in D_L , we are able to measure the number density fluctuation δ_{GW} over effectively the entire cosmic volume. This LSS is statistically anisotropic, since D_L^{obs} differs from its cosmological value D_L ,

$$D_L^{\text{obs}} = D_L(1 + 2\mathbf{v} \cdot \hat{n} - \kappa + \dots). \quad (1)$$

Here κ is the lensing convergence, describing the effect of gravitational lensing magnification. This effect is a highly valuable source of cosmological information (e.g. [8]). \mathbf{v} is the physical peculiar velocity [13] and \hat{n} is the line of sight unit vector. If an object is moving away from us ($\mathbf{v} \cdot \hat{n} > 0$), photons/GWs take longer time to reach us and suffer more cosmic dimming. At $z \gtrsim 1$, $\kappa \sim \mathcal{O}(10^{-2})$ and $\mathbf{v} \cdot \hat{n} \sim \mathcal{O}(10^{-3})$. Naively one would think the lensing effect overwhelms the peculiar velocity effect. This is indeed the case if we can subtract D_L

*Email me at: zhangpj@sjtu.edu.cn

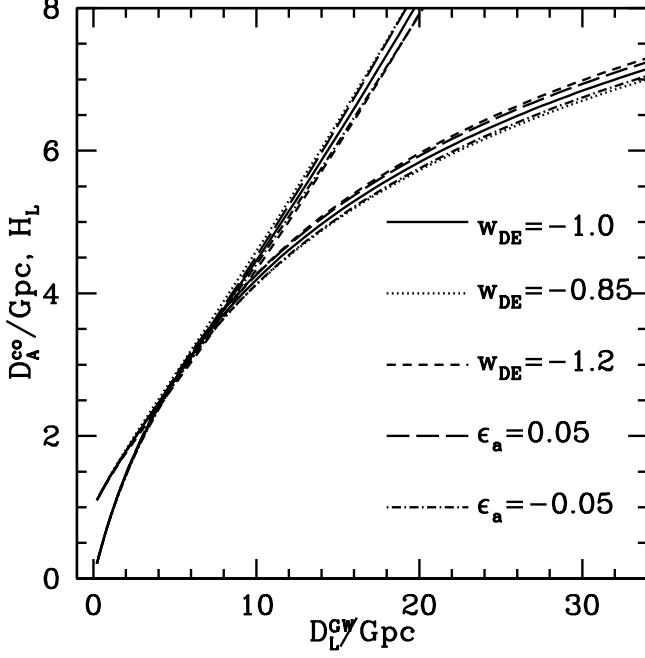


FIG. 1: The $D_L^{\text{GW}}-D_A^{\text{co}}$ and $D_L^{\text{GW}}-H_L$ relations. Like the $z-D_A^{\text{co}}$ relation and $z-H$ relations constrained by galaxy spectroscopic redshift surveys, the new set of relations is also sensitive to dark energy, demonstrated by the cases of various dark energy equation of state. A more unique application of these relations is to constrain modified gravity models in which $D_L^{\text{GW}} \neq D_L^{\text{EM}}$. We show two such cases, parameterized by $\epsilon_a = \pm 0.05$. Using GW alone, w_{DE} and ϵ_a constraints are largely degenerate. Combination with electromagnetic wave observations can break this degeneracy straightforwardly.

with cosmological redshift from spectroscopic follow-up. However, what affects the LDS LSS is the gradient of κ and $\mathbf{v} \cdot \hat{n}$ along the line of sight. Under the distance observer approximation and up to leading order, $\delta_{\text{GW}}^{\text{LDS}} \simeq \delta_{\text{GW}} + \alpha \nabla \kappa \cdot \hat{n} + \beta \nabla (\mathbf{v} \cdot \hat{n}) \cdot \hat{n}$. Since κ is lack of variation along the line of sight, its contribution is sub-dominant comparing to the velocity gradient contribution[29]. The LDS power spectrum then resembles the Kaiser [14] plus Finger of God formula in RSD,

$$P^{\text{LDS}}(k_{\perp}, k_{\parallel}) = P_g(k) \left(1 + \frac{f_L}{b_g} u^2\right)^2 F(k_{\parallel}). \quad (2)$$

Here $u \equiv k_{\parallel}/k$ and $k \equiv \sqrt{k_{\perp}^2 + k_{\parallel}^2}$. k_{\perp} (k_{\parallel}) is the wavevector perpendicular (parallel) to the line of sight. b_g is the density bias of GW host galaxies. $F(k_{\parallel})$ describes the FOG effect. There are two major differences to RSD. First,

$$f_L \equiv \left(\frac{2D_L/(1+z)}{d(D_L)/dz}\right) \times f. \quad (3)$$

It differs from $f \equiv d \ln D / d \ln a$ in RSD by a redshift dependent factor. This arises from the different effects

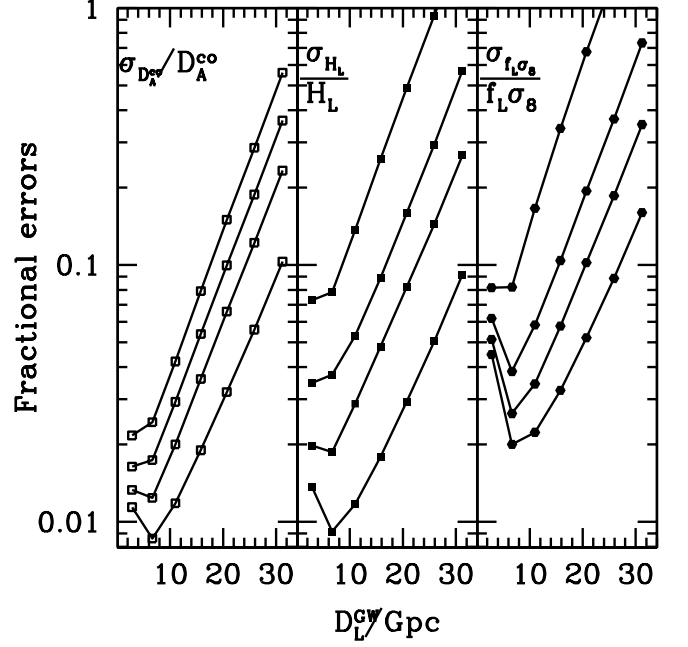


FIG. 2: The forecasted measurement errors on D_A^{co} , H_L and $f_L \sigma_8$ for a number of D_L^{GW} bins, assuming a ten year observation with a BBO-like experiment. These measurements can constrain dark energy (Fig. 1), or determine redshift adopting the distance duality. The distance measurement error σ_D is a major limiting factor. BBO can reach $\sigma_{\ln D} \sim 0.01$ for NS-NS mergers and ~ 0.001 for BH-BH mergers. Therefore we show the cases of $\sigma_{\ln D} = 0.02, 0.01, 0.005, 0.001$. σ_D degrades measurement of Fourier modes with $k_{\parallel} \gtrsim 0.04(0.01/\sigma_{\ln D})h/\text{Mpc}$.

of peculiar velocity on the luminosity distance ($D_L \rightarrow D_L(1 + 2\mathbf{v} \cdot \hat{n})$), and on redshift ($z \rightarrow z + \mathbf{v} \cdot \hat{n}(1 + z)$). The prefactor in Eq. 3 is zero at $z = 0$ and increases with z . It becomes larger than unity at $z \gtrsim 1.7$, where the peculiar velocity induced distortion is larger in LDS than in redshift space. The second difference is that the H factor shown up in FOG should be replaced by H_L .

Cosmological applications.— Now we proceed to constraints on D_A^{co} , H_L and $f_L \sigma_8$ using the LDS power spectrum measurement. Assuming Gaussian distribution in the power spectrum measurement errors, the Fisher matrix is

$$F_{\alpha\beta} = \sum_{\mathbf{k}} \frac{\partial P^{\text{LDS}}(\mathbf{k})}{\partial \lambda_{\alpha}} \sigma_P^{-2} \frac{\partial P^{\text{LDS}}(\mathbf{k})}{\partial \lambda_{\beta}}. \quad (4)$$

The sum is over \mathbf{k} bins. Instead of directly fitting D_A^{co} , $1/H_L$ and $f_L \sigma_8$, we fit their ratios ($A_{\perp}, A_{\parallel}, A_v$) with respect to the fiducial cosmology, along with b_g . Namely $\lambda = (A_{\perp}, A_{\parallel}, A_v, b_g)$. A_{\perp} (A_{\parallel}) scales the pair separation perpendicular (parallel) to the line of sight. Under such scaling,

$$P^{\text{LDS}}(k_{\perp}, k_{\parallel}) \rightarrow A_{\perp}^{-2} A_{\parallel}^{-1} P^{\text{LDS}}\left(\frac{k_{\perp}}{A_{\perp}}, \frac{k_{\parallel}}{A_{\parallel}}\right). \quad (5)$$

Statistical error σ_P in the power spectrum measurement is

$$\sigma_P = \sqrt{\frac{2}{N_{\mathbf{k}}}} \left[P^{\text{LDS}}(\mathbf{k}) + \frac{1}{\bar{n}_{\text{GW}}} W_{\parallel}^{-2}(k) W_{\perp}^{-2}(k) \right]. \quad (6)$$

$N_{\mathbf{k}}$ is the number of independent Fourier modes in the \mathbf{k} bin, proportional to the survey volume V_{survey} . W_{\parallel} (W_{\perp}) is the window function parallel(perpendicular) to the line of sight, due to statistical errors in the D_L measurement and angular positioning.

We adopt the fiducial cosmology as the Λ CDM cosmology with $\Omega_m = 0.268$, $\Omega_{\Lambda} = 1 - \Omega_m$, $\Omega_b = 0.044$, $h = 0.71$, $\sigma_8 = 0.83$ and $n_s = 0.96$. We are targeting at BBO or experiments of comparable capability. BBO has a positioning accuracy better than 1 arc-minute for all NS/BH-NS/BH mergers in the horizon [$k \lesssim 0.1h/\text{Mpc}$], $W_{\perp} = 1$ to excellent approximation. In contrast, $W_{\parallel} = \exp(-k^2 \chi^2 \sigma_{\ln D}^2 / 2)$ and the distance measurement error σ_D has a significant effect. For typical $z \sim 1$ and $\sigma_{\ln D} \sim 0.01$, the induced damping is significant at $k \gtrsim 0.03h/\text{Mpc}$. This limits the power spectrum measurement to the linear regime. On one hand, it reduces the constraining power. On the other hand, it simplifies the theoretical modeling, and allows us to neglect the FOG term in Eq. 2. \bar{n}_{GW} is the average number density of GW events in the survey volume. The local NS-NS merger rate is constrained to $R_0 = 1540_{-1220}^{+3200} \text{Gpc}^{-3} \text{year}^{-1}$ [4]. The BH-BH merger rate is a factor of ~ 10 smaller [15]. Therefore \bar{n}_{GW} is dominated by NS-NS mergers. For the evolution of NS-NS merger rate, we adopt the model in [7, 8]. For the bestfit R_0 , the total number of GW events per year is 0.33, 1.07, 1.77×10^6 at $z < 1, 2, 5$ respectively. We find that the luminosity-distance space LSS is capable of constraining D_A^{co} , H_L and $f_L \sigma_8$ in multiple D_L bins to a few percent accuracy (Fig. 2). These estimations adopt $\Delta t = 10$ years and $b_g = 1$. Since the power spectrum measurement error is shot noise dominated, the statistical errors roughly scale as $(R_0 \Delta t)^{-1} b_g^{-2}$. But their dependence on σ_D is more complicated. Fig. 2 shows the cases of $\sigma_{\ln D} = 0.005, 0.01, 0.02$, within the reach of BBO capability. σ_D has major impact on cosmology, by significantly affecting the number of accessible Fourier modes. For $\sigma_{\ln D} = 0.001$ which may be achieved by BH-BH merger observations of BBO or NS-NS mergers observations of more advanced experiments, cosmological constraints can be significantly improved, especially for H_L and $f_L \sigma_8$.

These constraints alone are able to constrain dark energy, demonstrated in Fig. 1. One way to under its constraining power is that, when the distance duality holds ($1 + z = D_L/D_A^{\text{co}}$), the D_L - D_A^{co} relation is equivalent to the more familiar z - D_L relation in the supernovae cosmology. It indeed contains valuable information of dark energy. However, due to lower number density and larger error in the D_L measurement, these constraints are significantly worse than what will be achieved by stage IV

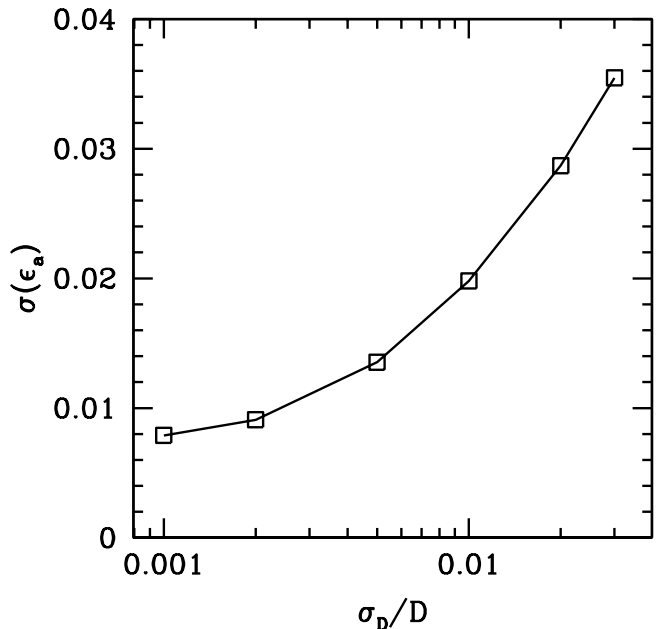


FIG. 3: Constraints on $D_L^{\text{GW}}/D_L^{\text{EM}}$, which is parametrized by a physically motivated parameter ϵ_a . This will put unique and powerful constraints on modified gravity models.

redshift surveys such as DESI [16] and Euclid [17].

Nevertheless, these measurements are unique in constraining modified gravity (MG) models. In these models, GW propagation may differ from electromagnetic wave propagation and $D_L^{\text{GW}} \neq D_L^{\text{EM}}$. This has been proposed and been applied to constrain gravity (e.g. [18, 19]). There are two degrees of freedom to modify the GW propagation equation [20]. One allows for deviation between the GW speed and the speed of light. However, GW170817 [4] has constrained the relative difference to be within $\mathcal{O}(10^{-15})$ [21], and ruled out a large fraction of MG models (e.g. [22]). In contrast, the other degree of freedom is essentially unconstrained. This is to modify the friction term in the GW propagation equation. [20] parametrizes this modification as $H(t) \rightarrow H(t)(1 - \delta(t))$. To avoid confusion of $\delta(t)$ with the commonly used LSS δ symbol, we adopt a different notation ϵ_{GW} . $\epsilon_{\text{GW}} \neq 0$ leads to

$$\eta \equiv \frac{D_L^{\text{GW}}}{D_L^{\text{EM}}} = \exp\left(-\int_0^z \frac{dz}{1+z} \epsilon_{\text{GW}}(z)\right) \neq 1. \quad (7)$$

Usually we expect no deviation from GR in the early epoch ($\epsilon_{\text{GW}}(a \rightarrow 0) \rightarrow 0$). A simple parameterization satisfying this condition is $\epsilon_{\text{GW}}(a) = \epsilon_a a$. Under this parameterization, $\eta = \exp(-\epsilon_a(1-a)) = \exp(-\epsilon_a z/(1+z))$.

Combining the z - D_A^{co} and/or z - D_L^{EM} measurements from electromagnetic wave telescopes, and the D_L^{GW} - D_A^{co} measurements here, we can measure $D_L^{\text{GW}}/D_L^{\text{EM}}$. Combining the z - H and D_L^{GW} - H_L measurements can also con-

strain this ratio. BBO can measure this ratio and constrain ϵ_a to percent level accuracy (Fig. 3). It will then be sensitive to MG models such as the RR model with $m^2 R \square^{-2} R$ correction in the action [20, 23]. Since this test of gravity is on the tensor part of space-time metric, it is highly complementary to tests on the scalar part. The statistical error here is dominated by the GW observations. $\sigma_{\ln D} \simeq 0.001$ will allow for better than 1% accuracy in ϵ_a , and longer observations can further help.

Further applications.— We point out that future GW experiments will map LSS in a new space, namely the luminosity-distance space (LDS), through the luminosity-distance determined using NS/BH-NS/BH mergers. We present a proof of concept study on its major LSS patterns (BAO and LDSD), and list a few cosmological applications (constraining dark energy, determining cosmological redshift and probing gravity). It has other applications. One is to probe the primordial non-Gaussianity. Another is to probe the horizon scale gravitational potential, since it alters the luminosity distance and generate a relativistic correction to the number density distribution of GW events. Both require the LSS measurement near the horizon scale. The LDS LSS is in particular suitable since it naturally covers the whole 4π sky and can extend to $z \gg 1$. Furthermore, the LDS LSS is free of all systematics associated with dust extinction, star confusion, masks and survey boundaries, due to the transparency of GWs. This will also make it advantageous in probing horizon scale LSS.

Including the cross correlation with the redshift space LSS overlapping in the survey volume, its power in constraining cosmology can be significantly enhanced. First, it will enable more accurate redshift determination, in a

way independent of galaxy clustering modelling and different to existing proposals [10–12]. Since galaxy surveys have $\mathcal{O}(10^2)$ higher number density, the constraint on $D_L^{\text{GW}}/D_L^{\text{EM}}$ (and ϵ_a) will be improved by $\mathcal{O}(10)$ than what shown in Fig. 3. This point will be addressed in a companion paper. Combining the LSS in the two spaces will also reduce cosmic variance in constraining primordial non-Gaussianity, gravitational potential and peculiar velocity, following the cosmic variance cancellation technique [24]. Furthermore, cross correlations between the luminosity-distance space and redshift space are also valuable for studies of stellar evolution and galaxy formation, such as constraining the NS/BH-galaxy relation. Notice that all these applications only require the overlap of GW observations and galaxy observations in cosmic volume. No spectroscopic follow-ups of GW events are required at all. Given the advance of DESI, Euclid, SKA and even more advance surveys [25], this requirement will be automatically satisfied. Given these potentials, we recommend more comprehensive studies of LSS in the luminosity-distance space.

Finally we address that the above proposal does not invalidate the usefulness of spectroscopic redshift follow-ups. With spectroscopic redshifts, the lensing field can be measured to high accuracy [8]. The velocity field, instead of the velocity gradient causing LDSD, can be determined as well [26]. Therefore massive spectroscopic follow-ups of GW events, although highly challenging, will be highly desirable as well.

Acknowledgement.— This work was supported by the National Science Foundation of China (11621303, 11433001, 11653003, 11320101002), and National Basic Research Program of China (2015CB85701).

-
- [1] B. P. Abbott, R. Abbott, T. D. Abbott, M. R. Abernathy, F. Acernese, K. Ackley, C. Adams, T. Adams, P. Addesso, R. X. Adhikari, et al., *Physical Review Letters* **116**, 061102 (2016), 1602.03837.
 - [2] B. P. Abbott, R. Abbott, T. D. Abbott, F. Acernese, K. Ackley, C. Adams, T. Adams, P. Addesso, R. X. Adhikari, V. B. Adya, et al., *Physical Review Letters* **118**, 221101 (2017), 1706.01812.
 - [3] B. P. Abbott, R. Abbott, T. D. Abbott, F. Acernese, K. Ackley, C. Adams, T. Adams, P. Addesso, R. X. Adhikari, V. B. Adya, et al., *Physical Review Letters* **119**, 141101 (2017), 1709.09660.
 - [4] B. P. Abbott, R. Abbott, T. D. Abbott, F. Acernese, K. Ackley, C. Adams, T. Adams, P. Addesso, R. X. Adhikari, V. B. Adya, et al., *Physical Review Letters* **119**, 161101 (2017), 1710.05832.
 - [5] B. F. Schutz, *Nature (London)* **323**, 310 (1986).
 - [6] B. P. Abbott, R. Abbott, T. D. Abbott, F. Acernese, K. Ackley, C. Adams, T. Adams, P. Addesso, R. X. Adhikari, V. B. Adya, et al., *Nature (London)* **551**, 85 (2017), 1710.05835.
 - [7] C. Cutler and J. Harms, *Phys. Rev. D* **73**, 042001 (2006), gr-qc/0511092.
 - [8] C. Cutler and D. E. Holz, *Phys. Rev. D* **80**, 104009 (2009), 0906.3752.
 - [9] T. Namikawa, A. Nishizawa, and A. Taruya, *Physical Review Letters* **116**, 121302 (2016), 1511.04638.
 - [10] M. Oguri, *Phys. Rev. D* **93**, 083511 (2016), 1603.02356.
 - [11] R. Nair, S. Bose, and T. D. Saini, *Phys. Rev. D* **98**, 023502 (2018), 1804.06085.
 - [12] S. Mukherjee and B. D. Wandelt, *ArXiv e-prints* (2018), 1808.06615.
 - [13] L. Hui and P. B. Greene, *Phys. Rev. D* **73**, 123526 (2006), astro-ph/0512159.
 - [14] N. Kaiser, *MNRAS* **227**, 1 (1987).
 - [15] B. P. Abbott, R. Abbott, T. D. Abbott, M. R. Abernathy, F. Acernese, K. Ackley, C. Adams, T. Adams, P. Addesso, R. X. Adhikari, et al., *Physical Review X* **6**, 041015 (2016), 1606.04856.
 - [16] DESI Collaboration, A. Aghamousa, J. Aguilar, S. Ahlen, S. Alam, L. E. Allen, C. Allende Prieto, J. Annis, S. Bailey, C. Balland, et al., *ArXiv e-prints* (2016), 1611.00036.
 - [17] L. Amendola, S. Appleby, A. Avgoustidis, D. Bacon, T. Baker, M. Baldi, N. Bartolo, A. Blanchard, C. Bonvin, S. Borgani, et al., *ArXiv e-prints* (2016), 1606.00180.

- [18] C. Deffayet and K. Menou, *ApJL* **668**, L143 (2007), 0709.0003.
- [19] K. Pardo, M. Fishbach, D. E. Holz, and D. N. Spergel, *JCAP* **7**, 048 (2018), 1801.08160.
- [20] E. Belgacem, Y. Dirian, S. Foffa, and M. Maggiore, *Phys. Rev. D* **97**, 104066 (2018), 1712.08108.
- [21] B. P. Abbott, R. Abbott, T. D. Abbott, F. Acernese, K. Ackley, C. Adams, T. Adams, P. Addesso, R. X. Adhikari, V. B. Adya, et al., *ApJL* **848**, L13 (2017), 1710.05834.
- [22] L. Amendola, M. Kunz, I. D. Saltas, and I. Sawicki, *Physical Review Letters* **120**, 131101 (2018), 1711.04825.
- [23] M. Maggiore, *Phys. Rev. D* **89**, 043008 (2014), 1307.3898.
- [24] P. McDonald and U. Seljak, *JCAP* **10**, 007 (2009), 0810.0323.
- [25] S. Dodelson, K. Heitmann, C. Hirata, K. Honscheid, A. Roodman, U. Seljak, A. Slosar, and M. Trodden, *ArXiv e-prints* (2016), 1604.07626.
- [26] P. Zhang and X. Chen, *Phys. Rev. D* **78**, 023006 (2008), 0710.1486.
- [27] X. Yang and P. Zhang, *MNRAS* **415**, 3485 (2011), 1105.2385.
- [28] https://tds.virgo-gw.eu/?call_file=ET0106C10.pdf
- [29] The area amplification of lensing adds an extra term -2κ to δ_{GW} . However, it is orders of magnitude smaller than the intrinsic clustering (e.g. [27]).